ACS SENSORS

Article

pubs.acs.org/acssensors

Glucose and Lactate Miniaturized Biosensors for SECM-Based High-Spatial Resolution Analysis: A Comparative Study

Alice Soldà,[†,‡] Giovanni Valenti,[†] Massimo Marcaccio,[†] Marco Giorgio,[‡] Pier Giuseppe Pelicci,[‡] Francesco Paolucci,*[,†] and Stefania Rapino*[,†,‡]

[†]Chemistry Department "Giacomo Ciamician", University of Bologna, Via Selmi 2, 40126 Bologna, Italy

[‡]Experimental Oncology Department, European Institute of Oncology, Via Adamello 16, 20139 Milan, Italy

Supporting Information

ABSTRACT: With the aim of developing miniaturized enzymatic biosensors suitable for *in vitro* diagnostic applications, such as monitoring of metabolites at single cell level, glucose and lactate biosensors were fabricated by immobilizing enzymes (glucose oxidase and lactate oxidase, respectively) on 10 μm Pt ultramicroelectrodes. These electrodes are meant to be employed as probes for scanning electrochemical microscopy (SECM), which is a unique technique for high-spatial-resolution electrochemical-based analysis. The use of enzymatic moieties improves sensitivity, time scale response, and information content of the microprobes; however, protein immobilization is a key step in the biosensor preparation that greatly affects the overall performance. A crucial aspect is the miniaturization of the sensing, preserving their sensitivity. In this work, we investigated the most common enzyme immobilization techniques. Several fabrication routes are reported and the main figures of merit, such as sensitivity, detection limit, response time, reproducibility, spatial resolution, biosensor efficiency, permeability, selectivity, and the ability to block electro-active interfering species, are investigated and compared. With the intent of using the microprobes for *in vitro* functional imaging of single living cells, we carefully evaluate the spatial resolution achieved by our modified electrodes on 2D SECM imaging. Metabolic activity of single MCF10A cells were obtained by monitoring the glucose concentrations in close proximity of single living cell, using the UME-based biosensor probes prepared. A voltage-switch approach was implemented to disentangle the topographical contribution of the cells enabling quantitative measurements of cellular uptakes.

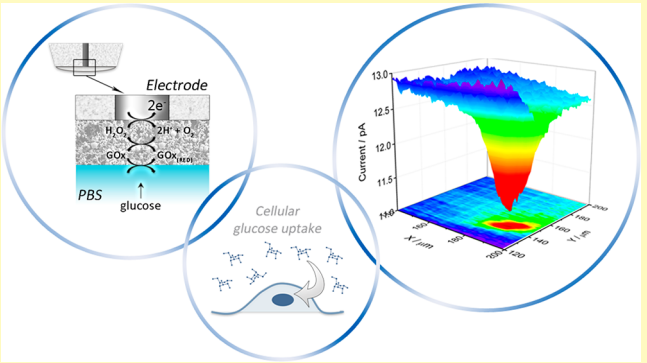

KEYWORDS: *glucose sensor, lactate sensor, microelectrodes, electrochemical modification, high-spatial resolution, SECM, single cell analysis*

In recent years, a large variety of miniaturized electrochemical sensors have been proposed, which are specifically developed for biomedical applications, such as monitoring of metabolites (e.g., glucose, lactate, glutamate, and ATP) of single living cells and measurement of the relevant kinetic parameters of the enzymatic processes involved; cellular respiration, metabolism, and protein synthesis were investigated employing electrochemical microbiosensors.[1,2] In such a context, scanning electrochemical microscopy (SECM) allows effective exploitation of the unique properties of such probes.[3] SECM employs ultramicroelectrodes (UMEs) that can be moved in the proximity of a surface while recording a faradaic current, which depends on both the topography and the electrochemical activity of the surface itself. Its versatility has been shown in a broad range of interdisciplinary applications[4] in sensors,[5] and for the investigation of biological systems.[1−6] A key feature of SECM in the latter applications is associated with its high temporal and spatial resolution (in the millisecond and micrometer scale, respectively) that allows in principle to scan the surface of a single living cell while electrochemically monitoring the activity associated with its metabolic changes.[7] In order to use a ultramicroelectrode based biosensor as a SECM probe, its physical-chemical features need to be optimized to obtain high sensitivity and low detection limits (from μM to nM), fast response time (0.1−1 s), and excellent spatial resolution (μm). Additionally, stability and reproducibility, easy manufacturing, and reduced costs are critical properties of sensors that need to be taken in consideration in the manufacturing procedure. Enzyme-based biosensors represent an important class of electrochemical probes suitable for single cell investigation by SECM. The optimization of the routes for the immobilization and miniaturization has largely been discussed[5,7,8] and applied to the detection of species with high spatial resolution in femtoliter volumes, e.g., for local detection in microenvironments[9] or for the development of

Received: May 14, 2017
Accepted: August 9, 2017

DOI: 10.1021/acssensors.7b00324
ACS Sens. XXXX, XXX, XXX−XXX

multisensor arrays,[10] or implantable or portable devices.[11] While the miniaturization brings some technical advantages such as steady state signals, fast response, reduced *iR*-drop, and an improved signal-to-noise ratio,[3,5] the reduced amount of immobilized biological recognition elements may lead to a limited sensitivity and loss of long-term stability, and requires further optimization of the biomolecule immobilization strategies.[12,13] Enzyme-based biosensors can be coupled with microfluidic systems to reduce the analyte volume (down to nanoliter) and to increase the sensitivity of the detection. The integration of microfluidic and micromanipulation apparatus and microelectrochemical detection has been demonstrated for gene function analyses,[14] for the detection of hormone active chemicals,[15] to develop biosensors for diabetes,[16] and for the detection of oxidative stress by macrophage cells.[17] Kueng et al. reported AFM-SECM biosensors for the investigation of glucose fluxes with a nanometric spatial resolution, they employed an electropolymerization method to address glucose oxidase transducing moieties at the AFM-SECM tip.[18] The highly spatial and topographical resolution of the AFM analyses was coupled with the amperometric information obtained from the enzymatic glucose biosensor. UME-based biosensor can be used with a simple SECM apparatus: this configuration led to a minor spatial resolution with respect to the nanobiosensor developed in the cited work,[18] but it is characterized by a good throughput capability which is fundamental in metabolic and diagnostic investigations. With reference to the important subclass of electrochemical biosensors based on oxidoreductases[13] and inspired by the pioneering work of Cliffel and coworkers,[7] herein we report on a comparative study of various fabrication protocols for the functional immobilization of either glucose oxidase (GOx: 160 kDa) or lactate oxidase (LOx: 50 kDa) and the development of UME-based biosensors for glucose and lactate, two important metabolites involved in the cellular metabolism. Fabrications protocols based on (i) covalent immobilization by cross-linking with glutaraldehyde; (ii) enzyme entrapment in polymer matrices (electropolymerization) using various polymers (i.e., poly (*o*-aminophenol) and polypyrrole); and (iii) adsorption through physical or electrostatic interactions (i.e., electrophoretic paints) were thoroughly investigated. Procedures and conditions were optimized in terms of sensitivity, limit of detection, linearity range, response time, stability, and reproducibility. Finally, in view of *in vitro* investigations of single cells by SECM, the spatial resolution achieved by the modified UMEs, the permeability of the enzymatic membranes, the selectivity, and the ability to block electroactive interference species were also carefully evaluated. The full characterization of the UME-based biosensors drove the choice for the most appropriate sensor in the investigation of single cell metabolism, demonstrated in the present work. Cell metabolism, and, in particular, glucose uptake, is one of the most important hallmarks of cancer;[19] the quantification of the glucose uptake at the single cell level is a powerful key enabling technology to elucidate cancer mechanisms and fostering early cancer diagnosis. In the present work, we implemented a voltage-switch approach,[6] employing a hydrophilic nontoxic redox mediator, to disentangle the topographical contribution of the cells: this enables the quantitative measurement of cellular uptake.

EXPERIMENTAL SECTION

Enzyme-Based UME Biosensors Fabrication. Enzyme coating layer was deposited onto 10 μm Pt UMEs via different methods.

Cross-Linking. The enzyme (8 mg/mL for GOx or 10 mg/mL for LOx) and BSA (62.5 mg/mL) were dissolved in PBS (pH 7.4) containing 0.02% v/v Triton X-100. After enzyme and BSA were thoroughly dissolved, 14 μL/mL buffer of 25% w/w GDA was added and quickly mixed.[7,20] It is mandatory to prepare a fresh solution for each biosensor because after a few hours the enzymatic solution turns to gel. The enzyme-based solution was hand-cast onto the surface of the UME by touching the tip of the UME with a tiny droplet of the solution. A thin layer adhered to the UME tip surface and it was let to air-dry for a couple of hours. Optimal drying time vary depending on temperature, humidity, and type of enzyme. The biosensors can be stored at RT until further use.

Electropolymerization. (i) With *o*-aminophenol: the enzyme (0.8 mg/mL for GOx or 2 mg/mL for LOx) and the o-AP monomer (0.55 mg/mL) were dissolved in 0.2 M acetate buffer pH 5.0. The solution was degassed by bubbling Ar for at least 10 min and the electrochemical polymerization of enzyme film was carried out by cycling in the potential range from 0.03 to 0.83 V at a scan rate of 50 mV/s. The film was grown for 15 cycles;[21] (ii) with pyrrole: the enzyme (0.5 mg/mL for GOx or 2.8 mg/mL for LOx) was dissolved in 0.1 M KCl pH 7.0 containing 0.05 M pyrrole. The solution is degassed by bubbling Ar for at least 10 min. Films were grown potentiostatically at 670 ± 5 mV for approximately 5 min.[22−24] The amount of charge transferred during electropolymerization was measured by online integration of anodic current according to Euler's method. The polymerization was stopped when the measured charge for surface area reached 45 mC/cm^2, for both UME and Pt arrandee polymerization.[23,24] The resulting enzyme-based electrodes were washed with MQ and stored in PBS at 4 °C until use.

Adsorption by Physical/Electrostatic Interactions. The enzyme (2 mg/mL for both GOx and LOx) was dissolved in MQ water and subsequently mixed with the cathodic Clearclad HRS EDP suspension (70 μL/mL, stock solution) and stored for 3 h at 4 °C. For enzyme/paint film formation, the cold preparation is transferred into the electrochemical cell and a potential-pulse profile (2.2 V for 0.2 s; 0.8 V for 1 s; 0 V for 5 s vs Ag/AgCl, 3 M KCl) was applied for 30 cycles, leading to the local generation of H^+ and concomitantly to the precipitation of the paint on the electrode surface which simultaneously entrapped the enzyme.[25] The modified electrodes were rinsed with MQ and stored before use 12 h in PBS at 4 °C.

Experimental methods and details on Chemicals and Materials used, Instrumentation, Amperometric Measurements, Cell Cultures, SECM Measurements, AFM Analysis, and details of the investigated immobilization protocols are fully described in Sections I and II of SI.

RESULTS AND DISCUSSION

In Figure 1, typical calibration chronoamperometric curves are reported for glucose (Figure 1A) and lactate (Figure 1B) UME biosensors, fabricated by the drop-casting method, as described in Section II of SI. A constant potential (E = +0.65 V) was applied at the modified UME and the current was continuously monitored while adding subsequent amounts of analyte, in the range from 0.01 to 1 mM. The current corresponds to the anodic oxidation of hydrogen peroxide, i.e., the secondary product of the catalytic reaction involving the enzyme entrapped at the electrode surface. The range of analyte concentrations was chosen in order to cover the expected values of extracellular environment concentrations, associated with metabolite uptake and efflux by single living cells.[7] Notice that, while the calibration plot for the GOx-based biosensor exhibits a linear behavior over the whole range of glucose concentrations (10 μM to 1 mM, Figure 1C), the LOx-based biosensor displayed two different linear regions, for [L-lactate] ≤ 0.4 mM and [L-lactate] ≥ 0.5 mM, respectively (Figure 1D). Such dual behavior was previously observed[7,26] and attributed to weak interactions between the entrapped enzyme and the electrode surface that would impair its activity at high substrate

DOI: 10.1021/acssensors.7b00324
ACS Sens. XXXX, XXX, XXX−XXX

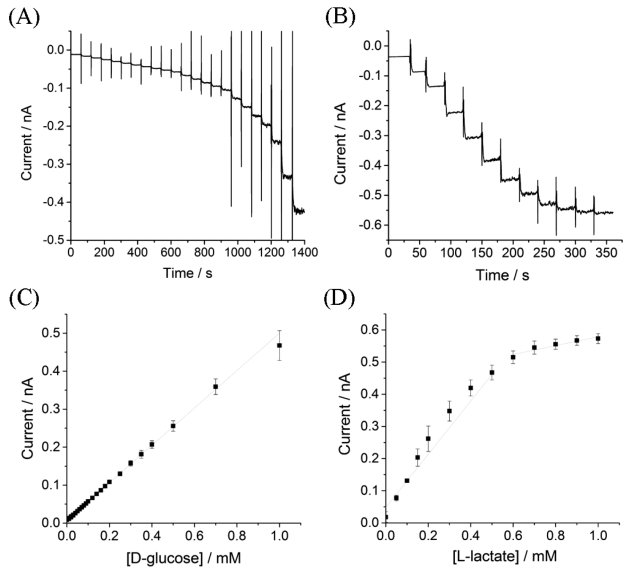

Figure 1. Representative amperometric calibration curves for drop-cast UME biosensor in PBS. E = +0.65 V vs Ag/AgCl, 3 M KCl. (A) GOx-based UME biosensor. Every current step corresponds to a single glucose concentration: 0.01, 0.02, 0.03, 0.04, 0.05, 0.06, 0.07, 0.08, 0.09, 0.1, 0.12, 0.14, 0.16, 0.18, 0.2, 0.25, 0.3, 0.35, 0.4, 0.5, 0.75, 1 mM. (B) LOx-based UME biosensor. Every current step corresponds to a single lactate concentration: 0.05, 0.1, 0.2, 0.3, 0.4, 0.5, 0.6, 0.7, 0.8, 0.9, 1 mM. Each value represents the mean value ± standard deviation of three experiments. Calibration plots of drop-cast (C) GOx- and (D) LOx-based UME biosensors.

concentrations. While a fairly linear Lineweaver−Burk double-reciprocal plot (Figure S1, Section III of SI) is observed anyway, this behavior would possibly be associated with an apparent dependence of the Michaelis−Menten (MM) constants on the substrate concentration. This would hold in the present enzyme working conditions as predicted by a theoretical model recently developed by us,[27] which describes the enzymatic kinetics in complex media and at very low analyte concentrations, where, i.e., one of the main hypotheses at the basis of MM equation derivation does not apply. Enzyme entrapment by electropolymerization or physical/electrostatic interactions (Table S1, Section II of SI), gave similar responses although with lower sensitivities and higher detection limit values (Figure S2, Section IV of SI). All the calibration curves, were analyzed to determine the apparent MM constant values (K_M^{App}), listed in Table 1. For more details, see Section V of SI.

Fabrication protocols and parameters providing best responses were identified by inspection of various figures of merit, that where eventually gathered in three main categories,[8] i.e., (i) analytical reliability (sensitivity, response time, selectivity, and permeability), (ii) analytical capacity (detection limits, linear range, and biosensor efficiency), and finally (iii) analytical variability (reproducibility and stability). Furthermore, in view of their application in electrochemical imaging of metabolic activities by SECM, also (iv) spatial resolution of all sensors was evaluated. The overall results are gathered in Table 1 and Table S2, Section VI of SI.

Analytical Reliability. For all biosensors, sensitivity was found to be increased with the coating thickness,[22] not unexpectedly since a thicker layer corresponds to larger amounts of entrapped enzyme. However, for thicknesses larger than 20 μm, the sensitivity was found to decrease again, as a likely consequence of significant hindering of diffusion of both substrate and hydrogen peroxide toward the electrode surface (Section VI of SI). The enzymatic activity is found to be inversely proportional to the GDA concentration used, because extensive cross-linking may result in a distortion of the enzyme structure (i.e., the active site conformation).[13] As a consequence, the accessibility and accommodation of the substrate may be reduced, thus affecting the retention of biological activity and the biosensor sensitivity.[12,13] The coverage with the active layer of the biosensors prepared by drop-casting, pyrrole and *o*-aminophenol electropolymerization methods results to be 8.13 pmol/cm^2, 13.8 pmol/cm^2, and 3.06 pmol/cm^2, respectively. The sensitivity of the biosensors seems not to be correlated with the surface coverage as the LOD of the drop-casting modified electrode is lower than the LODs obtained with both electropolymerized methods. The thickness and the morphology of the transduction films were characterized in order to better elucidate the influence of these features on the response time and sensibility of the different modification methods. Figure 2A,B shows the AFM images of the two layers obtained in tapping mode, which does not induce destructive frictional forces on the "soft" layer samples under investigation. In Figure 2C,D the AFM images and the corresponding section analysis are shown for the poly(*o*-aminophenol) and polypyrrole films, respectively, that have previously been scratched by the AFM tip to evaluate the film thickness. Thus, the average thickness of the enzymatic polymer layers was estimated to be around 25−30 nm and 15−20 nm for poly(*o*-aminophenol) and polypyrrole functionalization, respectively. Regarding the drop-cast method, we used scanning laser microscopy in reflection mode to study the thickness of the deposited enzymatic layer. Drop-cast UME electrodes with different time of immersion in the enzymatic solution were imaged (Figure S4, Section VII of SI). The results showed that the thickness of the layer was estimated to be equal to 0.47−0.58 μm after 3 min of immersion, equal to 0.74−0.76 μm (Figure 2) after 10 min of immersion and around 1−1.4 μm after 30 min of immersion. The active layer of the drop-cast method is 10-fold

Table 1. Analytical Parameters of Enzyme-Based UME Biosensor

immobilization method	enzyme	K_{MM}^{App}(mM)	sensitivity (mA/mM/cm^2)	response time (s)	LOD (μM)	linear range limit (mM)	reproducibility (% of standard deviation of the current response at 0.1 mM of analyte)
cross-linking: GDA	GOx	1.5 ± 0.5	1.16	3−6	10	4	22%
	LOx	0.17 ± 0.01	1.64	2−3	10	0.4	26%
poly (*o*-aminophenol)	GOx	4.3 ± 0.7	0.18	1−3	50	10	10%
	LOx	0.17 ± 0.01	0.20	1−2	50	0.2	18%
polypyrrole	GOx	4.1 ± 1.5	0.11	1−3	100	10	11%
	LOx	0.06 ± 0.02	0.16	1−2	50	0.2	13%
cathodic EDP	GOx	3.5 ± 0.8	0.03	5−8	100	5	30%
	LOx	0.04 ± 0.02	0.06	4−6	100	0.5	28%

DOI: 10.1021/acssensors.7b00324
ACS Sens. XXXX, XXX, XXX−XXX

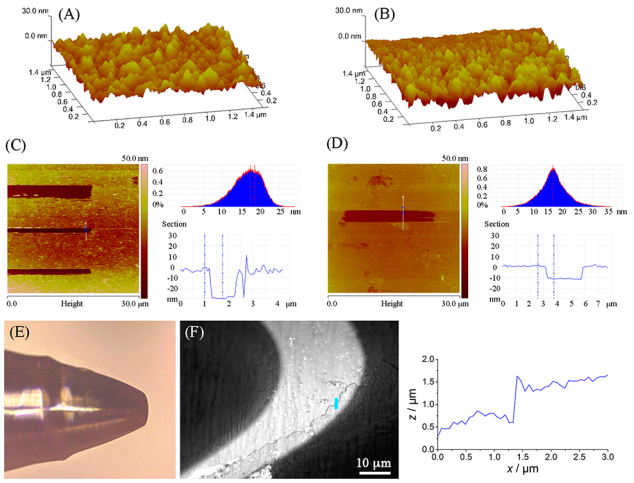

Figure 2. Tapping mode AFM images of the enzyme (GOx) entrapped into the (A) *o*-aminophenol and (B) pyrrole polymer matrix on platinum. (C) and (D) correspond to height images of the two methods, with the respective section analysis. (E) Laser scanning microscopy of a representative 10 min immersion drop-cast GOx-based UME biosensor with the (F) relative profile analysis: the blue bar represents the section area of the 2D profile.

thicker then the ones obtained with the electropolymerization methods. The thickness of the active layer likely affects the sensitivity of the UME biosensor as the drop-cast LOD is the lowest for the glucose detection. The thickness of the electropolymerized substrates cannot be increased up to the value of the drop-cast method as is limited by the accessibility of the electrode to the monomer.

The response time was also calculated (see Section VIII of SI) and it has been found to increase with the coating thickness as a consequence of larger diffusion times of the substrate. No effect was instead found in the response time of the system to direct H_2O_2 detection. The response time for biological applications should not exceed 10 s,[28−30] and therefore an optimal thickness should be selected to allow fast response coupled to a suitable sensitivity. As reported in Table 1, all the investigated fabrication protocols fulfilled the above criteria relative to the response time, with the fastest responses being associated, for both enzymes, to electropolymeric layers and the slowest to electrophoretic paints. The best compromise would then indicate electropolymerization method for GOx and cross-linking entrapment for LOx-based biosensor.

Selectivity was calculated for each GOx and LOx biosensor (details in Section IX of SI) in the presence of various interfering species commonly present in cell culture media, such as ascorbic acid, pyruvate, penicillin/streptomycin, insulin, glutamine, epidermal growth factor, and cholera toxin. Results, listed in Table 2, show that ascorbic acid (in the case of GOx-based sensors) and sodium pyruvate (for LOx-based sensors) may actively interfere with the detection of glucose and lactate since the ascorbic acid can be directly detected at the electrode at the working potentials of the biosensors. Sodium pyruvate may interfere with the LOx enzyme as it is the product of the catalyzed reaction. However, the sensitivity of the biosensors toward these interfering species are much lower compared to glucose and lactate. Moreover, the permeability of the sensing layer to the ultimate analyte (hydrogen peroxide) was calculated as the ratio between the analyte oxidation currents in either the absence or presence of the enzyme layer[31] (see Section X of SI). Drop-cast enzyme-based membranes (Table 2) displayed much lower permeabilities than electropolymerized membranes. In the latter case, values greater than 100% were observed: this behavior has been already reported for polymer layers containing a variety of macromolecular modifiers.[31,32] These values may be due to a minor disproportionation rate of hydrogen peroxide on bare Pt and its possible inhibition by polymer coatings.[33]

Analytical Capacity. Limit of detection (LOD) and linear range are among the most important criteria in order to evaluate the performance of a biosensors and the detection technique. All biosensors showed a linear response within a range that largely depended on the nature of enzyme and its immobilization method: the highest values of the linear range limit are 10 mM for GOx entrapped in electropolymerized membranes and 0.4−0.5 mM for LOx immobilized using drop-cast (GDA) or electrophoretic membranes (see Table 1). The lower linear range limit observed for LOx-based biosensors, with respect to GOx-based ones, is due to the intrinsically lower K_{MM} value of the free LOx enzyme. The covalent immobilization methods using GDA was found to yield much lower LODs than methods based on enzyme entrapment (electropolymerized and electrophoretic membranes) (see Table 1). The lower LOD obtained for the drop-cast method is also fostered by (i) the thicker transduction layer obtained employing drop-casting (vide Figure 2); (ii) the larger extension of the enzymatic layer for the drop-cast method in respect to the electropolymerization methods, as the entire surface of the UME probe (platinum active area and the surrounding insulating glass shield) is coated for the drop-cast method and only the active part of the electrode is functionalized for the electro-polymerization methods. In line with this result, the biosensor efficiency (BE%), i.e., the biosensor response to a specific analyte normalized to H_2O_2 signal at the same concentration,[31−33] was found to be significantly higher for drop-cast biosensors (20−30%) compared to the electropolymerized ones (1−3%) (Table 2). The enzymatic units entrapped using drop-cast methods are larger and, as a consequence, the enzymatic activity and

Table 2. Biosensor Efficiency, Permeability, and Selectivity Values for GOx and LOx-Based UME Biosensors

				permeability P(int)%		equimolar selectivity S%		substrate selectivity Ss%	
immobilization method	enzyme	BE%	permeability $P(H_2O_2)$%	(AA)	(Pyr)	(AA)	(Pyr)	(AA)	(Pyr)
GDA	GOx	32	27	2.7	N/A[a]	10.5	N/A[a]	33	N/A[a]
	LOx	23	44	1.6	23	0.96	0.16	0.42	0.72
poly (*o*-aminophenol)	GOx	2.7	144	6.8	N/A[a]	0.15	N/A[a]	5.3	N/A[a]
	LOx	0.63	119	1.9	120	0.03	0.04	0.54	6.8

[a]Not applicable, because enzyme-free designs do not respond to pyruvate. [b]100 μM of AA and 100 μM Pyruvate were considered for evaluating the interferences in respect to addition of the same amount of glucose and lactate. Only addition over 250 μM of AA interferes with lactate biosensor.

DOI: 10.1021/acssensors.7b00324
ACS Sens. XXXX, XXX, XXX−XXX

transduction are more efficient than for electropolymerized ones.

Analytical Variability. Reproducibility and stability were also assessed. The reproducibility of each type of biosensor was determined by measuring the current changes upon subsequent additions of substrate (up to 1 mM for glucose and 0.1 mM for lactate) as depicted in Table 1. As reported in the literature,[12] electropolymerized methods usually display a better reproducibility, likely because of the electrochemical control on deposition, whereas the casting procedure makes more difficult the control of exact amount of enzyme that gets deposited and, in particular, its homogeneity. Sensors prepared using different enzyme/polymer solutions and in different days were compared and their response was assessed: standard deviation of the signals obtained using electropolymerized membranes was around 10% and 18% for GOx- and LOx-based biosensors, respectively. For drop-cast and electrophoretic paint entrapment protocols, the standard deviation was larger, i.e., 22−26% and 30−28% for GOx- and LOx-based biosensors, respectively. The biosensor lifetime (stability) is clearly dependent on the nature of membranes and type of interaction of enzymes with the entrapping matrix. In the case of GDA cross-linked membranes, the sensitivity slightly decreased during the first 24 h (by 10%), but the biosensor response remained stable for at least 3 days. By contrast, electropolymerized membranes displayed improving performance during the first 24 h to 48 h of incubation in PBS likely associated with a rearrangement of enzymes inside the polymeric matrix, possibly due to a swelling of the film during incubation. Such sensors, properly stored in PBS at 4 °C, remained stable for days, up to 2 weeks (see Figure S10, Section XI of SI).

Spatial Resolution and Living Cell Investigation. A key advantage of using ultramicroelectrodes coupled with SECM is their ability to monitor microsystems, like, e.g., single living cells, with high spatial resolution (micro- or submicrometer range). Size, shape, and nature of the probing electrode, i.e, the thickness of the enzymatic coating and the overall dimensions of the UME biosensor, are important parameters determining the achievable spatial resolution.[18] The overall dimension of the UME biosensor and thickness of the enzymatic matrix should be in the micro- or submicrometer range, because the spatial resolution of SECM scales with the probe dimension. In order to investigate the UME-based biosensor performances on real samples we measured the glucose concentration in culture cell systems in the media in close proximity to single living cells. The cells investigated were MCF10A human breast epithelial cells. The proficiency in using UME-based biosensors and SECM to measure single cell glucose consumption was already shown by Cliffel group.[7]

By using approaches curves (ACs), the electrode is positioned at a known distance from the plastic bottom Petri dish on which cells are cultured (see Figure S11, Section XII of SI). The density of the culture was kept low to allow the imaging of single cells without any interference from neighboring ones. The tip−substrate separation distance was very accurately controlled by the feedback current response, the UME could be accurately moved and positioned using the piezo components and the stepper motors; furthermore, the probe vertical and horizontal movements were monitored simultaneously through the tip current and optical inspection by an inverted microscope to minimize any risk of damaging the enzymatic film of the biosensor during the experiment. The optical inspection also allowed to check the cell morphology. The ACs showed a typical negative feedback, due to hindered diffusion of glucose to the electrode with the decreasing of UME/dish distance. Following the approach step, the probe was retracted at the desired distance from the dish, and subsequently scanned horizontally above the cells to obtain the metabolic profiles associated with glucose uptake. The profiles are carried out in constant height mode. Prior and after each SECM measurements, calibration experiments were performed in order to check the correct UME-based biosensor performance (see Figure S12, Section XIII of SI).

Figure 3 shows typical profiles indicating that, as expected, on top of cells local concentrations of glucose decreases

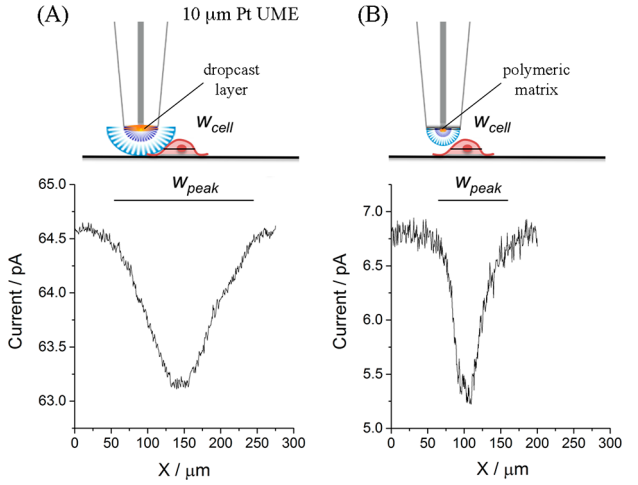

Figure 3. Schematic representation of the hemispherical diffusion around the active part of the drop-cast (A) and oAP electropolymerized (B) enzyme-based UME biosensor. Lower part: glucose uptake current profiles for a single MCF10A cell obtained in constant height mode. The scans were performed with dropcast (A) and electropolymerized (B) GOx-based 10 μm Pt UME biosensors. The experiment is carried out in PBS buffer containing glucose 0.1 mM, insulin 10 μM, and 2.5% of horse serum. Scan speed 15 μm/s. E = +0.65 V vs Ag/AgCl, 3 M KCl.

because of metabolic consumption. Two different fabrication methods are compared in Figure 3 and their spatial resolution was calculated as the ratio between the current peak width (w_{peak}) and the real cellular diameter (w_{cell}), which is around 30−60 μm for this cell line model. Using drop-cast biosensors, the widths of the peak is ranging between 150 and 230 μm, with a spatial resolution, calculated as w_{peak}/w_{cell}, around 5.4−5.7, for glucose and lactate analysis, respectively, whereas electropolymerized biosensors exhibit much narrower peaks, ranging between 70 and 125 μm and a spatial resolution around 1.2. Electropolymerization provides probes with ∼4 times higher spatial resolution than drop-cast membranes, as the current peak width is in the former case comparable to the real dimension of single cells. This is easily explained considering that, while electropolymerized membranes are spatially confined on the Pt disk, drop-cast ones cover both the active electrode area and the glass sheath, thus making the effective sensing area of the probe significantly large.

SECM Imaging of Glucose Uptake on Single Living Cells. 2D-images of the metabolic activity of single MCF10A cells were obtained by monitoring the glucose concentrations in close proximity of single living cell, using the probes prepared by the electropolymerization method. The choice of the

DOI: 10.1021/acssensors.7b00324
ACS Sens. XXXX, XXX, XXX−XXX

electropolymerized method was made in light of the previously demonstrated high spatial resolution. A culture of MCF10A was investigated employing UME-GOx/oAP biosensor and the glucose uptakes are shown in Figure 4. The current decrease in correspondence of the cells is associated with the metabolic consumption of glucose of each single cell. The spatial resolution of the UME-biosensor is suitable to discriminate the consumption of each single cell of the culture. Since the cell topography is not flat, the electrode−sample separation distance changes during the lateral scanning, affecting the diffusion of glucose to the sensor. As a consequence the current changes may also contain a topographical contribution. A quantitative measure of the glucose consumption cannot be achieved if this contribution is not disentangled. Various experimental approaches have been devised to single out the topographic contribution in SECM signals,[34] either based on coupled techniques, e.g., SECM-AFM,[18,35,36] SECM-shear-force,[37,38] or SECM-impedance,[39,40] or based on faradaic current-,[41] ion current-,[42] or electrochemical-[43,44] feedback distance-control. Most of the above approaches would, however, require additional probe modifications not totally compatible with the present biosensor architectures.

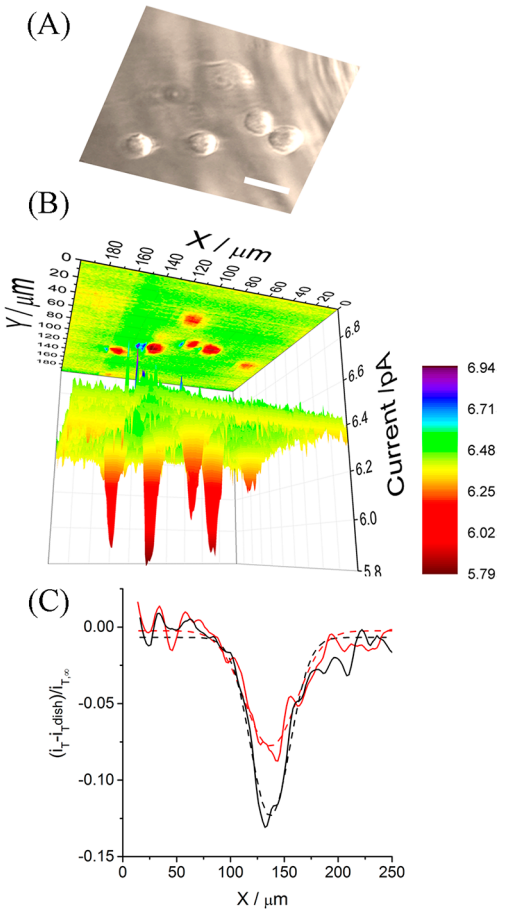

Figure 4. (A) Optical image of the scanned MCF10A cells. Scale bar: 30 μm. (B) Representative SECM image of glucose uptake of several MCF10A cells. SECM experiments were carried out in constant height mode using an electropolymerized 10 μm Pt GOx-UME biosensors in PBS buffer containing 0.1 mM glucose, 10 μM insulin, and 2.5% horse serum. Scan speed 15 μm/s. E = +0.65 V vs Ag/AgCl, 3 M KCl. Comparison between the two profiles: black line contains both functional and topographical contribution, while red line corresponds only to the topographical contribution. The currents were normalized by the respective steady-state bulk current values and subtracted by the normalized currents on the Petri dish. The measurements were performed with the same electropolymerized 10 μm Pt GOx-based UME biosensors in PBS buffer containing of glucose 0.1 mM, insulin 10 μM, and 500 μM of $[Ru(NH_3)_6]^{3+}$.

In the present work, in order to discriminate the topographic contribution from the functional response of living cells, a voltage-switching mode protocol was adopted.[45,46] This method is based on the subsequent acquisition of two separate signals via the SECM probe, the first relative to the analyte of interest (glucose in the present case), which contains both a functional and a topographical contribution, and a second one, obtained after the voltage switching, that is associated with the response of a secondary redox mediator and only contains ideally a topographical contribution.[45] After testing a variety of redox couples for their possible cytotoxicity, hexaaminoruthenium chloride, $[Ru(NH_3)_6]Cl_3$, was selected as redox mediator for the voltage-switching experiments. Such a redox couple has in fact a standard potential E° = −0.11 V vs Ag/AgCl, 3 M KCl, which is far enough from the potential used for hydrogen peroxide detection (E_{ox} = +0.65 V) to avoid any interference and, furthermore, such a species cannot cross the cell membrane thus assuring that only topographical effects (diffusion hindering) determine the current changes during the scans (Figure 4C). Ding and co-workers suggested that the overall current peak i_p is due to the sum of the component i_d caused by the negative feedback effect of the cell morphology and the contribution of the flux of the species through the cell membrane.[47] Thus, i_f, which corresponds to the contribution due to glucose flux of the living cell, can be calculated using $i_f = i_p - i_d$, where i_p was recorded at +0.65 V vs Ag/AgCl (glucose uptake and cell topography contributions) and the i_d contribution was assessed by the use of the ruthenium complex. The current contribution due to the glucose flux was then expressed as glucose concentration decrease by employing the calibration curve (see Supporting Information Section X). The absolute value of glucose concentration associated with the cellular uptake at single cell level has been estimated to be around 13 μM, in the case of the scan line reported in Figure 4C. Figure 4B shows a SECM 2D image of glucose uptake of a culture of MCF10A cells: from this result we can assess that each single cell is characterized by a glucose uptake profile and the profiles of the single cells are not overlapping. The average glucose uptake of the cells in Figure 4A,B is 17 ± 3 μM. Other methods for the deconvolution of topography and spatial physiological activity were reported,[48,49] and they can be employed, in conjunction with the herein described UME biosensors, for the quantitative study of cell metabolism. The glucose consumption of different cells of a layer can be easily coupled with (immuno) fluorescence imaging[8] to correlate specific protein expression to the cell metabolism, enabling the investigation of cancer mechanisms at single cell level.

CONCLUSIONS

Enzyme-based UME biosensors with practical interesting applicability in biology and medicine are typically characterized by very low limits of detection, very good response time, and easy and cheap manufacturing procedures. When such sensors are meant for SECM-based bioanalytical applications like, e.g., for the generation of 2D-images of the metabolic activity of single living cells, the above figures of merit need to be complemented by high spatial resolution. Upon reviewing some

DOI: 10.1021/acssensors.7b00324
ACS Sens. XXXX, XXX, XXX−XXX

of the major enzymatic immobilization methods in the literature, fabrication procedures and operational parameters were thoroughly analyzed in view of an optimized biosensor performance for diverse specific applications. So, for example, glutaraldehyde-based enzyme immobilization offers some desirable characteristics such as reproducibility, low cost, and easy fabrication, but provides probes with poor spatial resolution, stability, and selectivity with respect to those obtained, for instance, by electropolymerization. On the other hand, the latter biosensors are usually much less sensitive than those obtained by drop-casting, but possess a high spatial resolution (highest among the various classes herein investigated), in order to be very good probes for SECM investigations. Table 3, finally, gathers all information obtained

Table 3. Decision Matrix[a]

Criteria → / Protocols ↓	*Sensitivity LOD Biosensor Efficiency*	*Linear Range Response time*	*Spatial Resolution*	*Selectivity & Permeability*	*Reproducibility & Stability*
Crosslinking with GDA	+	=	=	−	=
Poly-*o*-aminophenol	−	+	+	=	+
Poly-pyrrole	−	+	+	=	+
Cathodic EDP	−	−	−	=	−

[a]Green cross means positive score for the criteria (thicker cross: very positive), yellow equal sign means comparable responses, and red line means negative score for the criteria of the several investigated protocols.

in the present study in the form of a decision matrix, whose scope is to serve as a practical tool for researchers to choose among the various fabrication methods the one that may better suit a specific biosensoristic application.

Employing Table 3, we selected the UME/poly-*o*-aminop-GOx biosensor for high spatial resolution functional imaging of a cell culture.

In conclusion, we demonstrated the real application of enzyme-based UME biosensor for single cell functional imaging in view of the following: (i) the resolution of the described method is proper for imaging single cell uptake profile in a cell culture; (ii) UME based biosensor serving as SECM probe can be used for the functional imaging of several cell of a culture in physiological conditions (living cells growth in adhesion) with a high-throughput capability. These features can be used both for the investigation of disease mechanisms such as cancer metabolism, to investigate the proficiency of drugs in cancer treatment, and for diagnostic application based on cell metabolism status and their metabolic response to external stimuli.

■ ASSOCIATED CONTENT

Supporting Information

The Supporting Information is available free of charge on the ACS Publications website at DOI: 10.1021/acssensors.7b00324.

Experimental methods and investigated protocols; Lineweaver−Burk plot for LOx-based UME biosensor; calibration curves obtained both for GOx- and LOx biosensor obtained by electropolymerization and electrophoretic deposition; MM constant calculation; evaluation of film thickness and the surface coverage; sensor selectivity, permeability, and stability; diffusion behavior of the Ru complex; typical AC and a representative calibration curve of the UME biosensor after SECM analysis (PDF)

■ AUTHOR INFORMATION

Corresponding Authors

*E-mail: francesco.paolucci@unibo.it. Tel: +39 051 2099460.
*E-mail: stefania.rapino3@unibo.it. Tel: +39 051 2099468.

ORCID

Giovanni Valenti: 0000-0002-6223-2072
Francesco Paolucci: 0000-0003-4614-8740
Stefania Rapino: 0000-0001-6913-0119

Notes

The authors declare no competing financial interest.

■ ACKNOWLEDGMENTS

We acknowledge the Italian Ministry of Health for GR-2011-02348455, Associazione Italiana per la Ricerca sul Cancro (AIRC), and the University of Bologna. A.S. acknowledges the Italian Foundation for Cancer Research (FIRC) for providing her the "Guglielmo Lucatello e Gino Mazzega" research fellowship.

■ REFERENCES

(1) Wittstock, G.; Horrocks, B. R. Biological System, In *Scanning Electrochemical Microscopy*, Bard, A. J.; Mirkin, M. V., Eds.; Marcel Dekker: New York, 2001; pp 445−512.

(2) Marcu, R.; Rapino, S.; Trinei, M.; Valenti, G.; Marcaccio, M.; Pelicci, P. G.; Paolucci, F.; Giorgio, M. Electrochemical study of hydrogen peroxide formation in isolated mitochondria. *Bioelectrochemistry* **2012**, *85*, 21−28.

(3) Bard, A. J. Introduction and principles, In *Scanning Electrochemical Microscopy*, Bard, A. J.; Mirkin, M. V., Eds.; Marcel Dekker: New York, 2001; pp 1−15.

(4) Mirkin, M. V.; Sun, P.; Laforge, F. O. Scanning electrochemical microscopy in the 21st century. *Phys. Chem. Chem. Phys.* **2007**, *9*, 802−823.

(5) Schuhmann, W.; Habermüller, K. Miniaturization of Biosensors, In *Electrochemical Microsystem Technologies*, Shultze, W.; Osaka, T.; Datta, M., Eds.; CRC Press, Taylor & Francis, 2002; pp 409−428.

(6) Rapino, S.; Marcu, R.; Bigi, A.; Soldà, A.; Marcaccio, M.; Paolucci, F.; Pelicci, P. G.; Giorgio, M. Scanning electro-chemical microscopy reveals cancer cell redox state. *Electrochim. Acta* **2015**, *179*, 65−73.

(7) Cliffel, D. E.; Ciobanu, M.; Taylor, D. E., Jr.; Wilburn, J. P. Glucose and Lactate Biosensors for Scanning Electrochemical Microscopy Imaging of Single Live Cells. *Anal. Chem.* **2008**, *80*, 2717−2727.

(8) Justino, C. I. L.; Rocha-Santos, T. A.; Duarte, A. C. Review of analytical figures of merit of sensors and biosensors in clinical applications. *TrAC, Trends Anal. Chem.* **2010**, *29*, 1172−1183.

(9) Whiteley, M.; Parsek, M. R.; Hmelo, L.; Wessel, A. K. Going local: technologies for exploring bacterial microenvironments. *Nat. Rev. Microbiol.* **2013**, *11*, 337−348.

(10) Ding, Z.; Henderson, J. D.; Li, M. S. M.; Filice, F. P. Three-Dimensional Electrochemical Functionality of an Interdigitated Array Electrode by Scanning Electrochemical Microscopy. *J. Phys. Chem. C* **2015**, *119*, 21473−21482.

(11) Watanabe, H.; Velmurugan, J.; Mirkin, M. V.; Svirsky, M. A.; Lalwani, A. K.; Llinas, R. R. Scanning Electrochemical Microscopy as a Novel Proximity Sensor for Atraumatic Cochlear Implant Insertion. *IEEE Trans. Biomed. Eng.* **2014**, *61*, 1822−1832.

DOI: 10.1021/acssensors.7b00324
ACS Sens. XXXX, XXX, XXX−XXX

(12) Marinesco, S.; Vasylieva, N. Enzyme Immobilization on Microelectrode Biosensors, In *Microelectrode Biosensors*, Marinesco, S.; Dale, N., Eds.; Humana Press c/o Springer Science, 2013; pp 95−114.
(13) Marinesco, S.; Frey, O. Microelectrode designs for oxidase-based biosensors, In *Microelectrode Biosensors*, Marinesco, S.; Dale, N., Eds.; Humana Press c/o Springer Science, 2013; pp 3−25.
(14) Yasukawa, T.; Nagamine, K.; Horiguchi, Y.; Shiku, H.; Koide, M.; Itayama, T.; Shiraishi, F.; Matsue, T. Electrophoretic cell manipulation and electrochemical gene-function analysis based on a yeast two-hybrid system in a microfluidic device. *Anal. Chem.* **2008**, *80*, 3722−3727.
(15) Ino, K.; Kitagawa, Y.; Watanabe, T.; Shiku, H.; Koide, M.; Itayama, T.; Yasukawa, T.; Matsue, T. Detection of hormone active chemicals using genetically engineered yeast cells and microfluidic devices with interdigitated array electrodes. *Electrophoresis* **2009**, *30*, 3406−3412.
(16) Pedraza, E.; Karajić, A.; Raoux, M.; Perrier, R.; Pirog, A.; Lebreton, F.; Arbault, S.; Gaitan, J.; Renaud, S.; Kuhn, A.; Lang, J. Guiding pancreatic beta cells to target electrodes in a whole-cell biosensor for diabetes. *Lab Chip* **2015**, *15*, 3880−3890.
(17) Amatore, C.; Arbault, S.; Chen, Y.; Crozatier, C.; Tapsoba, I. Electrochemical detection in a microfluidic device of oxidative stress generated by macrophage cells. *Lab Chip* **2007**, *7*, 233−238.
(18) Kueng, A.; Kranz, C.; Lugstein, A.; Bertagnolli, E.; Mizaikoff, B. Integrated AFM-SECM in tapping mode: Simultaneous topographical and electrochemical imaging of enzyme activity. *Angew. Chem., Int. Ed.* **2003**, *42*, 3238−3240.
(19) Koppenol, W. H.; Bounds, P. L.; Dang, C. H. Otto Warburg's contributions to current concepts of cancer metabolism. *Nat. Rev. Cancer* **2011**, *11*, 325−337.
(20) Cliffel, D. E.; Eklund, S. E.; Taylor, D. E., Jr.; Kozlov, E.; Prokop, A. A microphysiometer for simultaneous measurement of changes in extracellular glucose, lactate, oxygen, and acidification rate. *Anal. Chem.* **2004**, *76*, 519−527.
(21) Chen, J.; Pan, D.; Yao, S.; Nie, L.; Xia, J.; Tao, W. Amperometric glucose biosensor based on immobilization of glucose oxidase in electropolymerized *o*-aminophenol film at copper-modified gold electrode. *Sens. Actuators, B* **2005**, *104*, 68−74.
(22) Kim, H. S.; Shin, M. C. Electrochemical characterization of polypyrrole/glucose oxidase biosensor: Part I. Influence of enzyme concentration on the growth and properties of the film. *Biosens. Bioelectron.* **1996**, *11*, 161−169.
(23) Kim, H. S.; Shin, M. C. Electrochemical characterization of polypyrrole/glucose oxidase biosensor: Part II. Optimal preparation conditions for the biosensor. *Biosens. Bioelectron.* **1996**, *11*, 171−178.
(24) Adeloju, S. B.; Moline, A. N. Fabrication of ultra-thin polypyrrole-glucose oxidase film from supporting electrolyte monomer solution for potentiometric biosensing of glucose. *Biosens. Bioelectron.* **2001**, *16*, 133−139.
(25) Schuhmann, W.; Kurzawa, C.; Hengstenberg, A. Immobilization Method for the Preparation of Biosensors Based on pH Shift-Induced Deposition of Biomolecule-Containing Polymer Films. *Anal. Chem.* **2002**, *74*, 355−361.
(26) Horrocks, B. R.; Schmidtke, D.; Heller, A.; Bard, A. J. Scanning Electrochemical Microscopy. 24. Enzyme Ultramicroelectrodes for the Measurement of Hydrogen Peroxide at Surfaces. *Anal. Chem.* **1993**, *65*, 3605−3614.
(27) Bakalis, E.; Soldà, A.; Kosmas, M.; Rapino, S.; Zerbetto, F. Complex Media and Enzymatic Kinetics. *Anal. Chem.* **2016**, *88*, 5790−5796.
(28) Dale, N.; Llaudet, E.; Hatz, S.; Droniou, M. Microelectrode Biosensor for Real-Time Measurement of ATP in Biological Tissue. *Anal. Chem.* **2005**, *77*, 3267−3273.
(29) Dale, N.; Tian, F.; Gourine, A. V.; Huckstepp, R. T. A microelectrode biosensor for real time monitoring of l-glutamate release. *Anal. Chim. Acta* **2009**, *645*, 86−91.
(30) Amatore, C.; Lamaitre, F.; Meunier, A.; Bretou, M.; Darchen, F.; Collignon, M. G. Amperometric detection of vesicular exocytosis from BON cells at carbon fiber microelectrodes. *Electrochim. Acta* **2014**, *126*, 74−80.
(31) Rothwell, S. A.; Killoran, S. J.; O'Neill, R. D. Enzyme Immobilization Strategies and Electropolymerization Conditions to Control Sensitivity and Selectivity Parameters of a Polymer-Enzyme Composite Glucose Biosensor. *Sensors* **2010**, *10*, 6439−6462.
(32) Kirwan, S. M.; Rocchitta, G.; McMahon, C. P.; Craig, J. D.; Killoran, S. J.; O'Brien, K. B.; Serra, P. A.; Lowry, J. P.; O'Neill, R. D. Modifications of Poly(o-phenylenediamine) Permselective Layer on Pt-Ir for Biosensor Application in Neurochemical Monitoring. *Sensors* **2007**, *7*, 420−437.
(33) Harrar, J. E. Controlled-Potential Coulometric Determination of Hydrogen Peroxide. *Anal. Chem.* **1963**, *35*, 893−896.
(34) Wittstock, G.; Burchardt, M.; Pust, S. E.; Shen, Y.; Zhao, C. Scanning electrochemical microscopy for direct imaging of reaction rates. *Angew. Chem., Int. Ed.* **2007**, *46*, 1584−1617.
(35) Ueda, A.; Niwa, O.; Maruyama, K.; Shindo, Y.; Oka, K.; Suzuki, K. Neurite Imaging of Living PC12 Cells with Scanning Electrochemical/Near-Field Optical/Atomic Force Microscopy. *Angew. Chem., Int. Ed.* **2007**, *46*, 8238−8241.
(36) Macpherson, J. V.; Unwin, P. R. Combined Scanning Electrochemical−Atomic Force Microscopy. *Anal. Chem.* **2000**, *72*, 276−285.
(37) Lee, Y.; Ding, Z. F.; Bard, A. J. Combined Scanning Electrochemical/Optical Microscopy with Shear Force and Current Feedback. *Anal. Chem.* **2002**, *74*, 3634−3643.
(38) Schulte, A.; Nebel, M.; Schuhmann, W. Chapter twelve - Single Live Cell Topography and Activity Imaging with the Shear-Force-Based Constant-Distance Scanning Electrochemical Microscope. *Methods Enzymol.* **2012**, *504*, 237−254.
(39) Osbourn, D. M.; Sanger, R. H.; Smith, P. J. S. Determination of Single-Cell Oxygen Consumption with Impedance Feedback for Control of Sample-Probe Separation. *Anal. Chem.* **2005**, *77*, 6999−7004.
(40) Ding, Z. F.; Zhao, X. C.; Diakowski, P. M. Deconvoluting Topography and Spatial Physiological Activity of Live Macrophage Cells by Scanning Electrochemical Microscopy in Constant-Distance Mode. *Anal. Chem.* **2010**, *82*, 8371−8373.
(41) Laforge, F. O.; Velmurugan, J.; Wang, Y. X.; Mirkin, M. V. Nanoscale Imaging of Surface Topography and Reactivity with the Scanning Electrochemical Microscope. *Anal. Chem.* **2009**, *81*, 3143−3150.
(42) Takahashi, Y.; Shevchuk, A. I.; Novak, P.; Murakami, Y.; Shiku, H.; Korchev, Y. E.; Matsue, T. Simultaneous Noncontact Topography and Electrochemical Imaging by SECM/SICM Featuring Ion Current Feedback Regulation. *J. Am. Chem. Soc.* **2010**, *132*, 10118−10126.
(43) Takahashi, Y.; Shevchuk, A. I.; Novak, P.; Zhang, Y.; Ebejer, N.; Macpherson, J. V.; Unwin, P. R.; Pollard, A. J.; Roy, D.; Clifford, C. A.; Shiku, H.; Matsue, T.; Klenerman, D.; Korchev, Y. E. Topographical and electrochemical nanoscale imaging of living cells using voltage-switching mode scanning electrochemical microscopy. *Angew. Chem., Int. Ed.* **2011**, *50*, 9638−9642.
(44) Williams, C. G.; Edwards, J. W.; Colley, A. L.; Macpherson, J. V.; Unwin, P. R. Scanning Micropipet Contact Method for High-Resolution Imaging of Electrode Surface Redox Activity. *Anal. Chem.* **2009**, *81*, 2486−2495.
(45) Takahashi, Y.; Shevchuk, A. I.; Novak, P.; Babakinejad, B.; Macpherson, J.; Unwin, P. R.; Shiku, H.; Gorelik, J.; Klenerman, D.; Korchev, Y. E.; Matsue, T. Topographical and electrochemical nanoscale imaging of living cells using voltage-switching mode scanning electrochemical microscopy. *Proc. Natl. Acad. Sci. U. S. A.* **2012**, *109*, 11540−11545.
(46) Nebel, M.; Grützke, S.; Diab, N.; Schulte, A.; Schuhmann, W. Visualization of Oxygen Consumption of Single Living Cells by Scanning Electrochemical Microscopy: The Influence of the Faradaic Tip Reaction. *Angew. Chem., Int. Ed.* **2013**, *52*, 6335−6338.
(47) Xue, Y.; Lei, J.; Xu, X.; Ding, L.; Zhai, C.; Yan, F.; Ju, H. Real-time monitoring of cell viability by its nanoscale height change with

DOI: 10.1021/acssensors.7b00324
ACS Sens. XXXX, XXX, XXX−XXX

oxygen as endogenous indicator. *Chem. Commun. (Cambridge, U. K.)* **2010**, *46*, 7388−7390.
(48) Zhao, X.; Diakowski, P. M.; Ding, Z. Deconvoluting topography and spatial physiological activity of live macrophage cells by scanning electrochemical microscopy in constant-distance mode. *Anal. Chem.* **2010**, *82*, 8371−8373.
(49) Li, M. S. M.; Filice, F. P.; Ding, Z. A time course study of cadmium effect on membrane permeability of single human bladder cancer cells using scanning electrochemical microscopy. *J. Inorg. Biochem.* **2014**, *136*, 177.

DOI: 10.1021/acssensors.7b00324
ACS Sens. XXXX, XXX, XXX−XXX